# Time- and Frequency-domain Comparisons of the Wavepiston Wave Energy Converter

**Robert Read and Harry Bingham**
**Section for Fluid Mechanics, Coastal and Maritime Engineering**
**Department of Mechanical Engineering, Technical University of Denmark,**
**2800 Kgs. Lyngby, Denmark**
**rrea@mek.dtu.dk, hbb@mek.dtu.dk**

## Introduction

Analysis of wave-energy converters is most frequently undertaken in the time-domain. This formulation allows the direct inclusion of nonlinear time-varying loads such as power take-off (PTO) reactions, mooring forces, and viscous drag. However, integrating the governing equations of motion in the time domain is relatively computationally expensive, and requires a simulation to be conducted for each incident-wave state. In contrast, calculating the linearised performance of a wave energy converter (WEC) in sinusoidal waves of a given frequency is relatively inexpensive, albeit with the lower accuracy associated with the assumption of linearity. Combining this frequency-domain information with a spectral characterisation of the sea state therefore offers an opportunity to predict the power-capture performance of a WEC with less computational expense than a direct time-domain approach. In this regard, methods such as spectral domain linearisation (Folley, 2016) and nonlinear frequency domain analysis using a basis of trigonometric functions (Mérigaud and Ringwood, 2018) have been proposed to provide a compromise between speed and accuracy in assessments of WEC performance.

This paper will compare time- and frequency-domain analyses of the Wavepiston surging-plate WEC. This device consists of a surging plate close to the free surface that drives a staged telescopic hydraulic PTO. Modelling this system in the frequency domain presents challenges associated with the significant nonlinear forces arising from both the PTO reactions and the non-negligible viscous drag acting on the plate. Equivalent linear damping coefficients are used to model these forces in the frequency domain, while they are included explicitly in the time domain. The main idea of this paper is to quantify, for this device, the errors associated with linearising these two nonlinear processes. Our aim here is to assess the trade-offs between speed and accuracy when using a fully-linear frequency-domain approach compared to a partially-nonlinear time-domain method.

## Device description

This paper considers a surging-plate, attenuator-type WEC presently being developed by the Wavepiston company. A long steel cable is stretched between two floating buoys, typically several hundred metres apart, that are anchored to the sea bed. A pre-tension is applied so that the cable forms an essentially horizontal line located just below the free surface. Multiple plate modules are installed along the cable. A single module is illustrated in Figure 1, and consists of a moving plate element (shown in green) that can translate in surge relative to a stationary PTO unit (shown in red). The top of the plate is coincident with the undisturbed free surface, and waves propagate perpendicular to the plate surface. Energy is extracted from the wave by two telescopic hydraulic cylinders, one on either side of the plate. These cylinders, together with a system of check valves, alternately pump water from the sea into a transfer pipe that directs the flow to a turbine/generator system located onshore (see arrows in Figure 1(b)). This turbine system converts the wave energy to electricity with high efficiency whilst maintaining a pseudo-constant pressure inside the transfer pipe.

Results are here presented for a device configuration designed for optimal energy absorption at the DanWEC test site in Hanstholm, Denmark. The performance of a single plate module is considered. Here the moving plate element has a mass of 3600 kg and a plate area 6 m by 6 m. The dimensions of the hydraulic cylinders used in this test case are scaled versions of those specified for the smaller Wavepiston prototype currently deployed at DanWEC. The telescopic cylinders have three stages each. The internal diameters of the stages are 0.23 m, 0.27 m, and 0.34 m, with corresponding lengths of 3.00 m, 2.85 m, and 2.67 m respectively. A response of up to 8.52 m is thus permitted. Though not

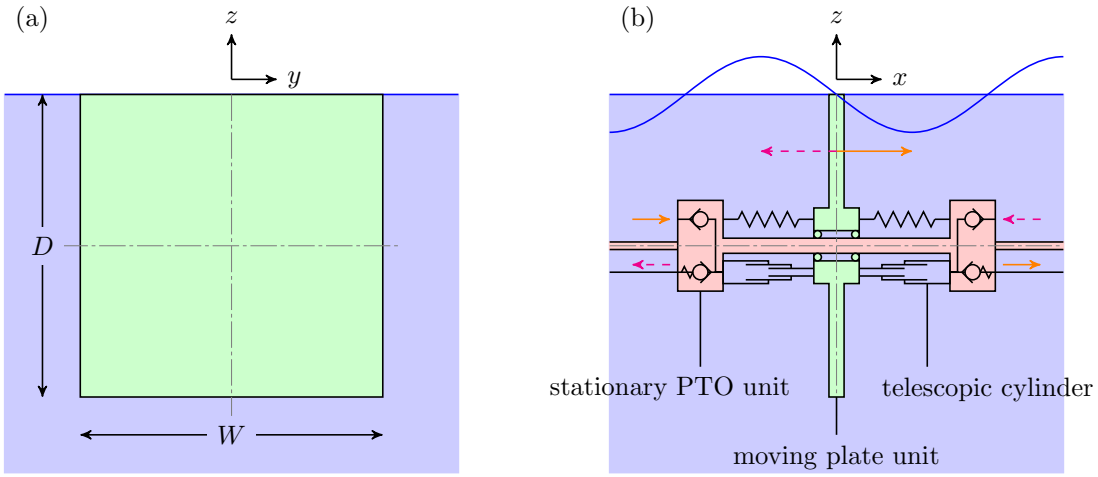


Figure 1: A plate module: (a) plate view from downwave; (b) plate and PTO view from side. Arrows indicate directions of plate motion and working-fluid flow.

present in the Wavepiston prototype, springs have been incorporated in the numerical PTO model to assess the full potential of the concept. A constant spring stiffness of $0.14\,\mathrm{MNm}^{-1}$ is utilised to generate resonance at the peak period corresponding to the most frequent wave condition at the test site. Although not true for the prototype design, where the pressure is limited, the numerical analysis assumes that the pressure in the transfer pipe can be set to an arbitrary, constant value to maximise the absorbed power for a given incident wave. Incorporating arbitrary pressure control into the numerical model again allows a better assessment of the concept's long-term potential.

## Mathematical modelling

### Frequency domain

The complex equation of motion in the frequency domain is formulated as

$$\left(-\omega^2\left(m+a\right)+\mathrm{i}\omega\left(b+b_\mathrm{v}+b_0\right)+c_0\right)\xi = F_\mathrm{d}+F_\mathrm{v}. \tag{1}$$

Here, $\xi$ is the plate response, while the added mass, $a$, the wave damping coefficient, $b$, and the wave diffraction force, $F_\mathrm{d}$, are obtained in the conventional manner using the linear boundary integral equation method as implemented in WAMIT (Lee and Newman, 2012). The time-varying viscous drag, generated as waves propagate past the plate, is significant and is estimated using the drag equation:

$$F_\mathrm{v}\left(t\right) = \frac{1}{2}\rho C_\mathrm{d}\int_{S_\mathrm{p}}\left|U_\mathrm{f}\right|U_\mathrm{f}\,\mathrm{d}s, \tag{2}$$

where $C_\mathrm{d}$ is the coefficient of drag (equal to 1.18 from White (1994)), $S_\mathrm{p}$ is the frontal area of the plate, and $U_\mathrm{f}$ is the component of the fluid velocity perpendicular to the plate. Integrating gives

$$F_\mathrm{v}\left(t\right) = \frac{\rho k C_\mathrm{d} W}{8}\left(\frac{gA}{\omega}\right)^2\left|\cos\theta\,\mathrm{Re}\left\{\mathrm{e}^{\mathrm{i}\omega t}\right\}\right|\cos\theta\,\mathrm{Re}\left\{\mathrm{e}^{\mathrm{i}\omega t}\right\}\frac{2kD+\sinh\left(2kh\right)+\sinh\left(2k\left(D-h\right)\right)}{\cosh^2\left(kh\right)}, \tag{3}$$

where $k$ is the wavenumber, $A$ is the wave amplitude, $\theta$ is the wave propagation angle, and $h$ is the water depth. For utilisation in the frequency domain, the drag can be re-expressed as a sinusoidal function that generates the same average power dissipation as the actual non-sinusoidal force. Thus, the surge viscous drag in Equation (1) can be represented as the real quantity

$$F_\mathrm{v} = \frac{1}{3\pi}\frac{\rho g C_\mathrm{d} W A^2}{\tanh\left(kh\right)}\left|\cos\theta\right|\cos\theta\frac{2kD+\sinh\left(2kh\right)+\sinh\left(2k\left(D-h\right)\right)}{\cosh^2\left(kh\right)}. \tag{4}$$

A viscous damping force is also generated solely due to motion of the plate through the surrounding water. An expression for the equivalent linear viscous damping coefficient included in Equation (1) can again be derived by ensuring that the average power transfer associated with the linear damping coefficient is equal to that associated with the actual nonlinear viscous drag. Thus,

$$b_{\mathrm{v}} = \frac{4}{3\pi}\rho\omega C_{\mathrm{d}} DW\left|\xi\right|. \tag{5}$$

The cylinder reaction at any time depends on the cross-sectional area of the cylinder experiencing displacement, and therefore varies in a step-wise manner with plate position. By again ensuring consistency in the average power transfer, the linear PTO damping coefficient is found to be given by

$$b_0 = -\frac{2}{\pi}\frac{p_{\mathrm{h}}}{\omega\left|\xi\right|}\sum_{i=1}^{N_{\mathrm{m}}} S_{\mathrm{h},i}\left[\cos\left(\omega t\right)\right]_{t_i}^{t_{i+1}}, \tag{6}$$

where $p_{\mathrm{h}}$ is the hydraulic pressure of the working fluid, $N_{\mathrm{m}}$ is the number of moving cylinder stages, and $S_{\mathrm{h},i}$ and $t_i$ are respectively the hydraulic area and transition time of stage number $i$.

Equation (1) has been solved for a range of regular wave conditions. In each case, $b_0$ is calculated using an optimisation function that maximises the power absorption while constraining the response to lie within the PTO's range of motion. Here, an iterative approach is required due to the interdependence of $b_{\mathrm{v}}$, $b_0$, and $\xi$. Having identified these variables, the average PTO power transfer is

$$P = \frac{1}{2}b_0\omega^2\left|\xi\right|^2. \tag{7}$$

The capture width ratio based on the plate width is then calculated in the normal manner as

$$\mathrm{CWR} = \frac{P}{{}^1\!/_2\rho g A^2 V_{\mathrm{g}} W}. \tag{8}$$

## Time domain

The equation of motion in the time domain is formulated as

$$\left(m + a^*\right)\ddot{\xi}\left(t\right) + \int_{-\infty}^{t} K\left(t-\tau\right)\dot{\xi}\left(\tau\right)\,\mathrm{d}\tau = F_{\mathrm{d}}\left(t\right) + F_0\left(t\right) + F_{\mathrm{v}}\left(t\right). \tag{9}$$

Here, in the classical manner proposed by Cummins (1962), the linear wave radiation force is characterised as the convolution of the surge radiation impulse response function, $K$, and the historical time series of the plate velocity, $\dot{\xi}\left(t\right)$. The linear wave diffraction force is modelled as the convolution of the diffraction impulse response function, $K_{\mathrm{d}}$, and the time series of the input surface elevation as follows,

$$F_{\mathrm{d}}\left(t\right) = \int_{-\infty}^{\infty} K_{\mathrm{d}}\left(t-\tau\right)\eta\left(\tau\right)\,\mathrm{d}\tau. \tag{10}$$

The nonlinear PTO force, $F_0\left(t\right)$, is evaluated exactly from knowledge of the plate position and its direction of travel, the telescopic cylinder geometry, and the working-fluid pressure obtained from the frequency-domain analysis. The total net viscous force in surge acting on the plate is also calculated exactly as

$$F_{\mathrm{v}}\left(t\right) = \frac{1}{2}\rho C_{\mathrm{d}}\int_{S_{\mathrm{p}}}\left|\dot{\xi}\left(t\right) - U_{\mathrm{f}}\right|\left(\dot{\xi}\left(t\right) - U_{\mathrm{f}}\right)\,\mathrm{d}s, \tag{11}$$

where $U_{\mathrm{f}}$ is the average wave-induced fluid velocity perpendicular to the plate's surface.

Equation (1) has been solved for a variety of regular wave conditions using the DTUMotionSimulator MATLAB package, the principles of which are described in Bingham (2000). Here, the hydrodynamic frequency response functions are read in from WAMIT output files and used, together with an input wave-elevation time series, to solve for the response at each time step. Time integration is performed using the classical fourth-order explicit Runge-Kutta method. Response constraints are also applied so that if the PTO range is exceeded, the plate position is reset to its maximum possible value and the velocity is set to zero. Having evaluated the response, the average absorbed power and capture width ratio are evaluated using Equations (7) and (8) respectively.

## Results for regular waves

Figure 2 shows how the capture width ratio varies with frequency for regular waves with two steepnesses. The points and lines correspond to time- and frequency-domain solutions respectively. Figure 2(a) shows a validation case where all viscous terms have been set to zero and an identical linear PTO damping has been applied in the time and frequency domains. As expected, these results are in good agreement. In Figure 2(b) viscous effects are again neglected, but the nonlinear PTO is represented exactly in the time domain. In this case, the time-domain CWR is lower than that predicted in the frequency domain between 1.0 $\text{rads}^{-1}$ and 2.5 $\text{rads}^{-1}$, though the agreement at resonance is good.

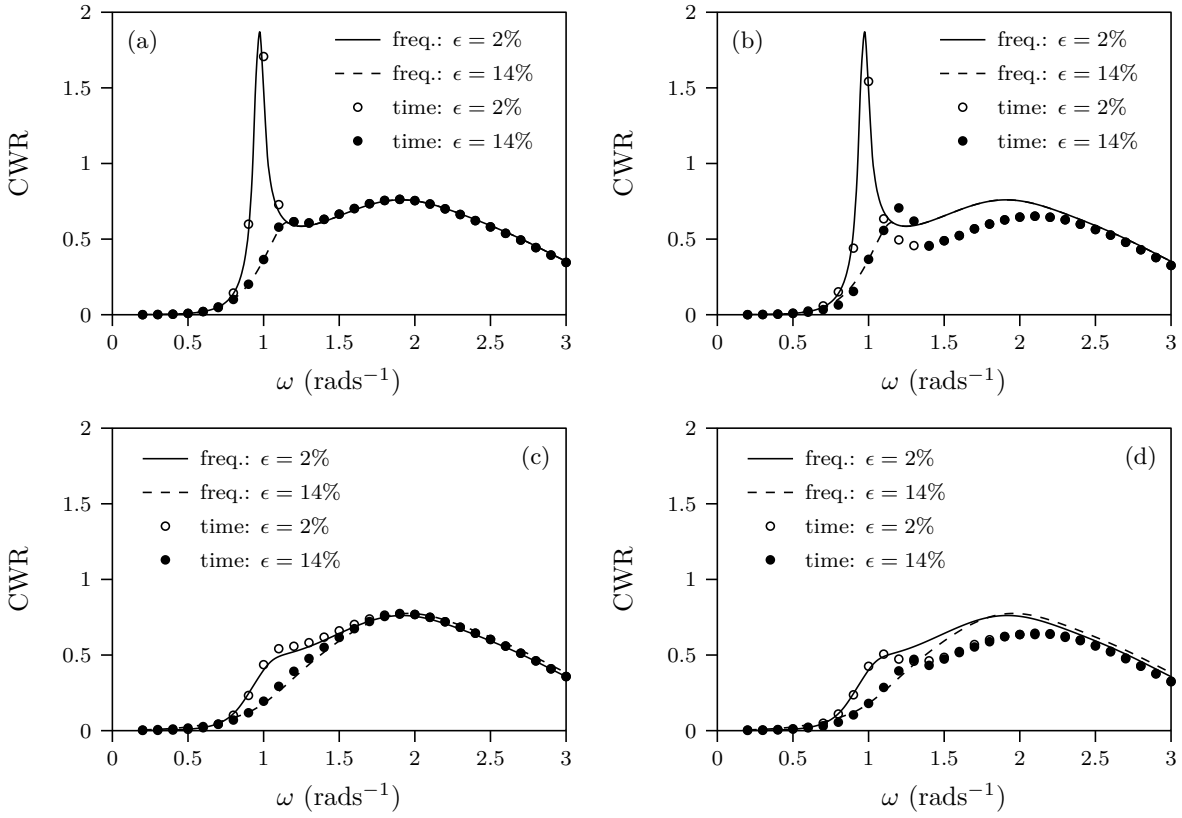


Figure 2: CWR: (a) inviscid, linear PTO; (b) inviscid, nonlinear PTO; (c) viscous, linear PTO; (d) viscous, nonlinear PTO.

Figure 2(c) shows results where the viscous drag on the plate has been included in the simulations, but a linear PTO damping has been applied. Correspondence between the results is good, but a significant reduction in CWR is apparent around the resonant point, particularly in the low-steepness case. The comparisons for the combined effects of nonlinear PTO and viscous drag are shown in Figure 2(d). Comparisons of the capture efficiency in irregular waves will be presented at the workshop.

## Acknowledgements

The authors wish to thank the Danish ForskEL programme for their generous financial support and the Wavepiston company for their technical guidance.

H. B. Bingham. A hybrid boussinesq-panel method for predicting the motion of a moored ship. *Coastal Engineering*, 40(1), 2000.

W. E. Cummins. The impulse response function and ship motions. Technical Report 1661, Department of the Navy: David Taylor Model Basin, October 1962.

M. Folley, editor. *Numerical Modelling of Wave Energy Converters*. Academic Press, 2016.

C.-H. Lee and J. N. Newman. WAMIT User Manual Version 7.0, 2012. http://www.wamit.com/manual.htm.

A Mérigaud and J. V. Ringwood. A nonlinear frequency-domain approach for numerical simulation of wave energy converters. *IEEE Transactions on Sustainable Energy*, 9(1):86–94, 2018.

F. M. White. *Fluid Mechanics*. McGraw-Hill, third edition, 1994.